

**KANSAS GEOLOGICAL SURVEY  
OPEN-FILE REPORT 97-10**

MULTI-CHANNEL ANALYSIS OF SURFACE WAVES (MASW):  
A Summary Report  
of Technical Aspects, Experimental Results, and Perspectives

by

Choon B. Park  
Richard D. Miller  
Jianghai Xia

*Disclaimer*

The Kansas Geological Survey does not guarantee this document to be free from errors or inaccuracies and disclaims any responsibility or liability for interpretations based on data used in the production of this document or decisions based thereon. This report is intended to make results of research available at the earliest possible date, but is not intended to constitute final or formal publications.

Kansas Geological Survey  
1930 Constant Avenue  
University of Kansas  
Lawrence, KS 66047-3726

# **Multi-Channel Analysis of Surface Waves (MASW)**

**"A summary report of technical aspects, experimental results, and perspective"**

prepared by

Choon B. Park  
Richard D. Miller  
and  
Jianghai Xia

of the

**Kansas Geological Survey**

January, 1997

Open-file Report #97-10

## INTRODUCTION

When seismic waves are generated at or near the surface of earth, both body (P and S)- and surface (e.g., Rayleigh, Love, etc.)-waves are generated. Body waves propagate through the whole body of the earth, whereas surface waves along (or near) the surface of the earth. If vertical seismic sources are used, the type of generated surface-waves is Rayleigh waves, more-commonly called ground roll in seismic surveys. In exploration and engineering seismology, ground roll has been treated as the most troublesome noise masking the useful body wavefields. Most of efforts have been made to attenuate it through data acquisition and processing techniques (Lombardi, 1955; Anstey, 1986; Knapp, 1986).

Surface-waves, however, have dispersion property that body-waves lack. This property is that different wavelength has different penetration depth and, therefore, propagates with different velocity. Therefore, by analyzing the dispersion of surface waves, one can obtain near-surface velocity profile. It is the shear (S)-wave velocity ( $v_s$ ) profile that is obtained by analyzing ground roll. The entire procedure of the analysis consists of three steps: acquisition of dispersive ground roll data, construction of the dispersion curve, and backcalculation (inversion) of S-wave velocities from the constructed dispersion curve. The accurate construction of the dispersion curve is the most critical because the final product of  $v_s$  profile has the accuracy that depends solely upon the accuracy of the dispersion curve.

In all kinds of surface seismic surveys using vertical sources, ground roll takes more than two thirds of total generated seismic energy and usually appears with the most prominence on the multi-channel records. Therefore, generation and recording of ground roll is easiest among all other types of seismic waves.

Shear (S)-wave velocity ( $v_s$ ) profile obtained from the ground-roll analysis can find many useful applications. First of all, because the shear-wave velocity is directly proportional to shear modulus that is in turn a direct indicator of stiffness (or rigidity) of material, the  $v_s$  profile can be used as a near-surface stiffness profile, evaluation of which, in geotechnical engineering, has been one of the critically important tasks. The so-called deflection-response method (Lytton et al., 1975) in that area evaluates the stiffness by measuring stress-strain behavior of the materials caused by static or dynamic load. This method, however, measures the overall stiffness of a site and each individual layers cannot be measured. Furthermore, evaluation of a large-area geotechnical site by this method can be time-consuming, expensive, and even damaging to many surface points. The crosshole and downhole method of wave-propagation to measure the stiffness can also be time-consuming, expensive, and destructive to the site because it requires drilling of borehole(s) and installation of receivers (and sources) in borehole(s). The stiffness profile from the ground-roll analysis, on the other hand, can provide the stiffness of each subsurface layers in nondestructive and fast fashion.

The  $v_s$  profile obtained from the ground-roll analysis can be used to detect (or resolve) near-surface features that are hard to be detected even by the high-resolution reflection method that

has been used increasingly since 1980 in engineering, environmental, and groundwater projects. The high-resolution reflection method often fails to be effective in such cases as when the near-surface target is beyond resolution limit (e.g., vertically or near-vertically fractured or collapsed zone) or when the target is underlain by (or embedded in) highly heterogeneous and absorptive materials (e.g., mapping the interface between the bedrock and overburden that consists of highly absorptive and heterogeneous materials). In these cases, the target may cause a characteristic dispersion property of ground roll. Therefore, it is possible in these cases not only to detect but also to resolve the targets on the calculated  $v_s$  profile. Continuous survey of ground roll can make it possible to image near-surface heterogeneity caused by the anomalous zones through proper design of field technique and effective handling of obtained surface wave data.

In early 1980's, a wave-propagation method to generate the near-surface  $v_s$  profile, called Spectral Analysis of Surface Waves (SASW), was introduced (Nazarian and Stokoe, 1983) that makes use of spectral analysis of ground roll generated from impact sources like hammers on the surface. The method has been widely and effectively used in many geotechnical engineering projects. Usually only two receivers (geophones) are used and the spacings between the receivers and receiver and source are changed many times to cover the desired range of investigation depth. Because of this necessity of the repeated tests, it usually takes several hours to complete the whole procedure at one test site.

Multi-Channel Analysis of Surface Waves (MASW) is a fast method of evaluating near-surface  $v_s$  profile because the entire range of investigation depth is covered by one or a few generation of ground roll without changing receiver configuration. Furthermore, the inclusion of noise wavefields such as body waves (direct, refracted, reflected, and air waves) (Sanchez-Salinero et al., 1987) and reflected (Sheu et al., 1988) and higher-modes (Gucunski and Woods, 1991) ground roll can be identified by their different coherency in arrival times on a multi-channel record and can be handled properly by various kinds of multi-channel data processing techniques to improve the accuracy of the results from the analysis. Among all types of these body waves is the strong first arrivals (refraction events) most troublesome. Inclusion of nonplanar Rayleigh waves (Sanchez-Salinero et al., 1987) that can lead to errors can also be identified and handled properly during the analysis. As a whole, the multi-channel recording method makes the quality control during data acquisition and processing steps more effective than by SASW method.

On a Vibroseis uncorrelated record, all the characteristics of ground roll can be identified on the level of each single frequency component because each individual frequency component is represented in isolation with other components. This makes the quality control even more efficient. Furthermore, an accurate and fast coherency measure, called Cross-Correlation of Stacked Amplitudes with Sweep (CCSAS) (Park et al., 1996b) can be used to construct the dispersion curve.

## SURFACE-WAVE METHOD OF $v_s$ PROFILING

In general, there are two types of surface waves most widely observed in seismic prospecting and earthquake seismology; Rayleigh and Love waves (Dobrin and Savit, 1988). Ground roll is Rayleigh-type surface waves generated most effectively in all kinds of surface seismic surveys using vertical seismic sources. More than two thirds of seismic energy generated are imparted to ground roll (Heisey et al., 1982). Theoretically, both types of the surface waves are predicted by certain form of the plane-wave solutions to the following coupled elastic wave equation (Haskell, 1953):

$$\frac{\partial^2 \Phi}{\partial t^2} = v_p^2 \nabla^2 \Phi \quad \text{and} \quad \frac{\partial^2 \Psi}{\partial t^2} = v_s^2 \nabla^2 \Psi,$$

where  $\Phi$  and  $\Psi$  represent displacement potentials, and  $v_p$  and  $v_s$  represent P- and S-wave velocities. Rayleigh waves have particles motion in vertical direction, whereas Love waves have particles motion in horizontal direction. Because their particle motion is always horizontal, Love waves are seldom recorded during most seismic surveying in which only vertical source and receivers are used.

In a layered medium in which seismic velocity changes with depth, both types of the surface waves have dispersion property, that is indicative of elastic moduli of near-surface earth materials: different wavelength has different penetration depth and propagates with different velocity. Short wavelength has shallow penetration and longer one has deeper penetration. The propagation velocity for each wavelength, called phase velocity (Bath, 1973), depends primarily on the shear (S)-wave velocity ( $v_s$ ) of the medium over the penetration depth and is influenced only slightly by the compressional (P)-wave velocity, density ( $\rho$ ), and Poisson's ratio ( $\sigma$ ). Therefore, the surface-wave velocity is a good indicator of  $v_s$ . It is normally assumed the phase velocity of ground roll is about 92 percent of  $v_s$  (Stokoe et al., 1994), and the ratio changes between 0.88 and 0.95 for the entire range of Poisson's ratio (0. - 0.5) (Ewing et al., 1957). Theoretical values for the phase velocities of different wavelengths can be found by solving the above elastic wave equation with boundary conditions set by the layered model (Haskell, 1953).

Therefore, by analyzing the dispersion feature of ground roll represented in recorded seismic data, the near-surface S-wave velocity ( $V_s$ ) profiles can be constructed and the corresponding shear moduli ( $\mu$ ) are calculated from the relation between the two parameters:

$$v_s = \sqrt{\frac{\mu}{\rho}}, \quad \text{or} \quad \mu = v_s^2 \rho$$

where  $\rho$  represents density of material. Change of density with depth is usually small in comparison to the change in  $\mu$  and is normally ignored or guessed. With known (or guessed) Poisson's ratio, one can also obtain P-wave velocity ( $v_p$ ) profile from  $v_s$  profile.

The entire procedure of generating  $v_s$  profile consists of three steps: acquiring ground roll data in the field, processing the data to determine dispersion curve (a plot of frequency vs. phase velocity), and backcalculation of the  $v_s$  for different depths. The wavefields of horizontally traveling ground roll are recorded by receivers (geophones) laid at the surface with certain spacing  $dx$ . Recorded wavefields are then analyzed at different frequencies ( $f$ ) for the phase velocities ( $C_f$ ) based upon the difference ( $\Delta t_f$ ) in the arrival times of ground roll at two receivers as

$$C_f = \frac{dx}{\Delta t_f}.$$

This analysis produces a set of data ( $f$  vs.  $C_f$ ), the dispersion data, that are in turn passed into next step of analysis, the inversion process. The inversion process backcalculates S-wave velocity ( $v_s$ ) profile from the measured dispersion data. Two different approaches are possible for inversion: forward modeling and least-squares algorithm. The forward modeling involves assuming a  $v_s$  profile, and then comparing the theoretical dispersion curve with the empirical (Stokoe et al., 1994). The assumed profile is modified until the two curves match closely.

The least-squares algorithm seeks the  $v_s$  profile whose dispersion curve matches best with the empirical curve in least-squares sense (Nazarian, 1984; Sanchez-Salinerio et al., 1987; Rix and Leipski, 1991). It is an automated, but computationally intensive method.

## **DISPERSION CURVE**

Dispersion curve is a plot of a data set consisting of frequencies and phase velocities. The  $v_s$  profile is determined based upon this dispersion curve. Therefore, accurate determination of dispersion curve is the most critical part affecting the accuracy of  $v_s$  profile.

### **MULTI-CHANNEL ANALYSIS OF SURFACE WAVES (MASW)**

vs.

### **SPECTRAL ANALYSIS OF SURFACE WAVES (SASW)**

In general, there are two methods that make use of Rayleigh-wave dispersion property for the purpose of generating near-surface  $v_s$  profile: Spectral Analysis of Surface Waves (SASW) method introduced by Stokoe and his coworkers at University of Texas Austin and Multi-

Channel Analysis of Surface Waves (MASW) developed at Kansas Geological Survey (KGS) (Park et al., 1996a; 1997a).

SASW method uses only two receivers to record ground roll that is usually generated by impact source like sledge hammer, and, therefore, the test needs to be repeated with many different field setups (different source and receiver spacings) to cover different depths of investigation (Figure 1a). The test is also performed in two directions to cover effect of any internal phase shifts due to receivers and instrumentation (Nazarian et al., 1983). The necessity of the repeated tests also exists for the purpose of reducing the influence of random noise. Collected data are analyzed to determine dispersion curve based upon cross-spectral phase and coherence by use of a spectrum analyzer (Stokoe et al., 1994). The method is time and labor intensive due to the necessity of repeated tests with different field configurations. It usually takes several hours to complete the entire process. Furthermore, since only two receivers are used, all possible adverse effects cannot be detected and handled properly that may cause errors in the results. These effects are the inclusion of body waves (direct, refracted, reflected P-waves, and air waves), and higher-modes, reflected, and nonplanar surface waves. Because of this, quality control during the acquisition and processing periods is extremely difficult and the accuracy of the results can be significantly reduced.

In MASW method, multiple number (usually twelve or more) of receivers with so-many-channel seismograph are used (Figure 1b). Receivers are planted with equal spacing and either single geophone or a group of multiple geophones can be used as a receiver. Because basic field configuration is very similar to that for body-wave surveying only with slightly different criterion on the optimum data-acquisition configuration (Park et al., 1996c), the surface-wave survey can be performed as a by-product of body-wave surveying, making 100 percent of recorded seismic energy useful. Even when a separate surveying with unfavorable configurations for body-wave recording is essential, the recorded body wavefields will not be useless for the surface-wave analysis.

Two types of MASW method have been developed at KGS: multi-channel analysis of surface waves using Vibroseis (MASWV) (Park et al., 1996c) and multi-channel analysis of surface waves using impulsive source (MASWI) (Park et al., 1997a). Each type has difference in type of source used and data processing technique to generate dispersion curve. MASWV uses a swept source like Vibroseis and MASWI uses an impulsive source like sledge hammer. The data processing techniques are a time-domain approach for MASWV (Park et al., 1996b) and a frequency-domain approach for MASWI (Park et al., 1997a).

In MASW method, recorded multi-channel Vibroseis data in uncorrelated format are analyzed in the field to determine dispersion curve. Various types of multi-channel data processing techniques may be used for this purpose (Herrmann, 1973; McMechan and Yedlin, 1981; Mari, 1984; Mokhtar et al., 1988). However, cross-correlation of stacked amplitude with sweep (CCSAS) method by Park et al. (1996b) provides excellent accuracy and speed. When this method is employed, the entire process including inversion step usually takes less than fifteen minutes after field setup for the 48-channel record of 12-s record length with 1 ms sampling interval if 66 Mhz Intel 486-based PC is used.

## **MASW USING VIBROSEIS (MASWV)**

Surface-wave (ground roll) data were collected at the Kansas Geological Survey test site using IVI Mini-Vibrois. Main purpose of testing was to collect ground roll data with distinctive dispersion character. The site consists of a thick ( $> 50$  m) formation of shale layers overlying a sequence of Kansas cyclothem (Moore, 1964). Surface topography had a slight upward bulge with maximum bulge less than 1 m. The procedure to come up with optimum acquisition parameters outlined in Park et al. (1996c) was followed.

48-channel Geometrics Strataview seismograph was used with 10-Hz Mark-Product geophones, but only 41 channels were used with first channel dedicated to recording sweep. Three clustered geophones formed one receiver group. The receiver spacing was 1 m. The source offset was 27 m. Sampling interval was 1 ms with total sweep and listening times of 10 s and 2 s, respectively. A sweep of 10 Hz - 50 Hz was used.

Figure 2 shows uncorrelated raw field record. One record has total record length of 12000 ms (12 s) and is displayed in 1500-ms segments. On top of each display is shown the sweep frequency at the beginning of each segment, whereas at bottom is shown the recording time at the end of each segment. Below this display of uncorrelated record is the field configuration schematically illustrated. Due to the tapering, full-amplitude sinusoidal waves appear only after 0.5 s.

Ground roll with a good coherency is observed throughout most of the sweep frequencies. Dispersive character of ground roll is apparent as noticed by change in slope with sweep frequency. However, at high ( $> 40$  Hz) frequencies the attenuation of ground roll is so severe that the body-wavefields (refractions) start to dominate the record. This effect always starts to appear from the far-offset traces and spreads into the near-offset traces. The effect is therefore called far-offset effect. Velocity of the body-wavefields is about 1600 m/s as calculated from a correlated record.

Phase velocities are calculated from the record shown in Figure 2 by using Cross-Correlation of Stacked Amplitudes with Sweep (CCSAS) method. Range of calculated frequency was from 12 Hz to 50 Hz. 12-Hz is the lowest frequency with full amplitude generated by the source. The constructed dispersion curve (Figure 3b) shows a realistic trend that matches with the trend of the dispersion curve constructed manually by measuring slopes of ground roll for many different frequencies. The manually calculated phase velocity for 50 Hz could be calculated from the ground roll event noticeable after 10 s on the displayed section. The dispersion curve constructed by using CCSAS method shows the phase velocities at highest frequencies match with this manually calculated value. This indicates CCSAS method has an excellent capability of tolerating the inclusion of strong body wavefields.

The dispersion curve in Figure 3b was inverted to produce near-surface shear-wave velocity ( $v_s$ ) profile by using an algorithm by Xia et al. (1997). The profile is shown in Figure 3a in comparison with a  $v_s$  profile constructed from a down-hole shear-wave survey conducted at

the test site. The dispersion curve corresponding to the inverted  $v_s$  profile is shown in Figure 3b in comparison with the observed dispersion curve. The inverted  $v_s$  profile matches with the down-hole  $v_s$  profile with a high accuracy.

### **MASW USING IMPULSIVE SOURCE (MASWI)**

The method of multi-channel analysis of surface waves using impulsive source (MASWI) is a similar method to MASWV method. Two main differences are, however, in type of the source used and the data processing technique to generate dispersion curve. Instead of a swept source like Vibroseis, an impulsive source like a sledge hammer is used. The data processing technique is a frequency-domain technique, instead of a time-domain technique of CCSAS in MASWV method, similar to the spectral analysis technique used in SASW method. The technique, however, does not involve calculation of phase difference of recorded surface waves that is the case in SASW method. The calculation of phase difference is prone to generate erroneous results because of the so-called wraparound phenomenon. Instead, the technique calculates phase velocities based upon a spectral correlation parameter (Park et al., 1997a). Therefore, the calculated dispersion curve can have much a greater confidence than that calculated by SASW method. Computational speed of this technique is also faster than those of MASWV and SASW techniques.

Because of the type of source used, MASWI method is much a cheaper, simpler, and faster method than MASWV method. However, there can be two main drawbacks in comparison to MASWV method. First, it is very difficult in MASWI method to control the spectral contents of the generated surface waves. In consequence, bandwidth of recorded surface waves is often narrower than that by MASWV method. This narrowness can significantly limit maximum investigation depth and the resolution within the investigatable depth range (Rix et al., 1991). Second, the data processing technique to generate dispersion curve tends to have slightly less tolerance for the inclusion of body waves than the technique (CCSAS) used in MASWV method. This drawback in data processing, however, is currently being investigated thoroughly and expected to be alleviated soon. Efforts are also being made to alleviate the first drawback of MASWI method by examining various types of impulsive source with various conditions near the impact point.

Figure 4 shows construction of dispersion curve by using the data processing technique developed for MASWI method. The input data used was not an impulsive data but the correlated record of a Vibroseis record. The main purpose of displaying this figure is to show the robustness of the technique that generates a highly comparable result to that by CCSAS method MASWV.

### **IMAGING METHOD**

Shear-wave velocity ( $v_s$ ) profile has been the main product one can benefit from the analysis of surface waves. The background principle in this way of utilizing surface waves is based

upon the dispersion property of surface waves: different wavelengths penetrate different depths of earth and corresponding phase velocities represent elastic property of earth within the penetrating depths. Therefore, if the dispersion property is measured not only over a small horizontal surface distance covered by one receiver line, but also over a large distance surveyed by continuously moving the source-receiver setup, one can obtain the change in elastic property of near-surface with both depth and horizontal distance. It seems that there can be many possible ways of analyzing and displaying the two-dimensional elastic property of earth from this continuous surface-wave survey. The first method we developed is described below.

In this method, multi-channel field records are obtained with source-receiver setup moving horizontally in a regular fashion. For example, if one field record is obtained with source at  $x_s^1$  and receivers at  $xr_k^1$  ( $k = 1, \dots, N$ ), then next field record is obtained with  $x_s^2 = x_s^1 + dx$  and  $xr_k^2 = xr_k^1 + dx$ . Vibroseis is used as source and one common sweep is used throughout the entire survey. All the obtained field records are then sorted into common-receiver gathers. Linear moveout (LMO) correction is applied to all these gathers using one common velocity function.

The velocity function dictates the velocity (phase velocity) of a particular sweep frequency component in a gather. Therefore, after LMO correction, the sloping feature of surface waves for all frequencies should be removed and the surface waves events now become flat events. Because one common velocity function is used, the surface wave events after the correction will become flat only if the corresponding near-surface has the same velocity model as the one used for the correction. Otherwise, the events will not be perfectly flattened (Figures 6 and 7).

After LMO correction, all the traces in a gather are stacked to make one stacked trace. The final stacked section then comprises of these stacked traces in the order of receiver locations. Large amplitudes at a particular point in this stacked section indicate the near-surface velocity being close to the value in the velocity function used during LMO correction, whereas small amplitudes indicate the near-surface velocity being different. Therefore, the image created by this pattern of amplitude difference represents the image of the variation of the near-surface velocity that in turn is related to the image of the near-surface heterogeneity.

Figures 5 and 6 show a modeling of the imaging method described above. Earth model consists of horizontally homogeneous velocity model except for a rectangular abnormally. The velocity models for both normal and abnormal zones are shown in Figure 5a. The anomaly zone has lower velocity than ambient part of the earth. Attenuation property of the earth was modeled in such a way that attenuation is most severe at the shallowest depths and mild at deep depths, and the anomaly zone has severer attenuation than the ambient zones. The stacked section shown in Figure 8 clearly shows the existence of the anomaly zone as "white" spot where amplitudes are smallest at the depth range that approximately matches with the model. The approximate depth is calculated with the assumption that penetration depth is about half

wavelength. The "white" image is created mainly by the anomaly in velocity and partially by the anomaly in attenuation property.

The imaging method was tested in the field where the main feature of the near-surface anomaly exists as a underground steam tunnel buried underneath a soccer field in campus of Kansas University in Lawrence, Kansas. Survey line was designed to pass over the tunnel in perpendicular direction. Size of the tunnel is 1 m by 2 m at 2 m depth.

About 100 field records were acquired by continuously moving the source-receiver setup, starting from the surface location well ahead of the surface location of the tunnel and ending the survey when the source location passed over the surface location of the tunnel.

Figure 9 shows the stacked section obtained by following the procedure outlined previously. The existence of the tunnel is obvious. Some other near-surface anomalies at depths shallower than the tunnel are also seen. These anomalies are believed to represent the existence of heterogeneity such as sidewalk, tree roots, and some buried bulky objects.

## **DISCUSSIONS AND CONCLUSIONS**

Main difference between SASW and MASW lies in both field technique and data processing technique to generate dispersion curve. Obviously, MASW is much a faster and simpler method because of its multi-channel recording that eliminates the necessity of repeated measurements by changing field configuration. Furthermore, the generation of dispersion curve in MASW method seems to maintain robustness because of its unique ways of calculating phase velocity that are based upon as much objective facts as possible. Comparison of the two methods through modeling justified these advantages of MASW method over SASW method. Direct comparison of the two methods through real experiment will be executed soon.

Because of the simplicity in data acquisition and processing, it is possible to automate the entire procedure as much as possible. As the research progresses, it is expected that an accurate  $v_p$  profile can be produced within five minutes after start of data acquisition with as much less human involvement as possible. Under such circumstances where an approximate method of inversion can be used instead of using a full matrix inversion method, the profile can be generated in less than one minute.

When a continuous profiling of near-surface materials over a certain surface range is necessary in the form of either  $v_p$  profile or image section of heterogeneity, it will be possible to generate the result in real-time mode. Especially when a receiver platform (Figure 10) is employed (this is currently under investigation), the survey would be able to proceed with progressive generation of the results in a similar speed and fashion as ground probing radar (GPR) method would do.

Currently, research directions at KGS are focused into following categories:

1. Refinement of both field acquisition and data processing techniques to further increase the speed and accuracy in final result
2. Development of imaging method by using impulsive source like a sledge hammer
3. Emphasis on the refinement of impulsive method in both  $v_s$  profiling and imaging
4. Development of tomographic imaging method

Category 4 may need a special comment. Basic principle of tomographic imaging is to accurately estimate property (e.g., elastic or electromagnetic property of earth) of a certain part of medium by having redundancy in measurement (e.g., travel time or attenuation). Mathematically speaking, the estimation is accomplished by solving a overdetermined inversion matrix (Santamarina, 1994). Inversion of surface wave data has an inherent property of reduced resolution and accuracy with depth (Rix et al., 1991). All surface-seismic methods (e.g., refraction or reflection method) suffer from this drawback. To alleviate this drawback in MASW method, certain part of near-surface where more accurate estimation at depth is required, surface-wave surveying can be performed by changing azimuthal angle of source-receiver line (Figure 11). In this case, it is possible to construct an overdetermined system of linear equations to be solved for more accurate value of elastic parameter at depth.

Based upon all the research results by far, followings are concluded on MASW method:

- MASW is an efficient method of investigating elastic property of near-surface materials.
- It is efficient because of its high accuracy that is achieved by both special field technique and data processing technique.
- It is efficient because of its fast speed of accomplishing necessary results.
- MASW makes it possible to produce not only quantitative display of near-surface elastic property in the form of  $v_s$  profile but also qualitative display of the image of near-surface heterogeneity.
- MASW is a method that can be fully automated to investigate elastic property of near-surface materials for the usage in various engineering fields.

## REFERENCES

- Anstey, N. A., 1986, Whatever happened to ground roll?: *The Leading Edge*, 5(3), 40-45.
- Båth, M., 1973, *Introduction to seismology: A Halsted Press Book*, 395 pp.
- Bullen, K. E., 1963, *An introduction to the theory of seismology: Cambridge At The University Press*, 381 pp.
- Burger, H. R., 1992, *Exploration geophysics of the shallow subsurface: Prentice Hall, Inc., Englewood, NJ*, 489 pp.
- Dobrin, M. B., and Savit, C. H., 1988, *Introduction to geophysical prospecting, 4th ed.: McGraw-Hill, Inc.*, 867 pp.
- Gucunski, N., and Woods, R. D., 1991, Instrumentation for SASW testing, *in Geotechnical special publication no. 29, Recent advances in instrumentation, data acquisition and testing in soil dynamics*, edited by S. K. Bhatia, S. K. and G. W. Blaney, American Society of Civil Engineers, 1-16.
- Ewing, W. M., and Jardetzky, W. S., 1957, *Elastic waves in layered media: McGraw-Hill, Inc.*, 380 pp.
- Haskell, N. A., 1953, The dispersion of surface waves on multilayered media: *SSA Bull.*, 43, 17-34.
- Heisey, J. S., Stokoe II, K. H., and Meyer, A. H., 1982, Moduli of pavement systems from spectral analysis of surface waves: *Transportation Research Record No. 852*, 22-31.
- Herrmann, R. B., 1973, Some aspects of band-pass filtering of surface waves: *SSA Bull.*, 63, 663-671.
- Lombardi, L. V., 1955, Notes on the use of multiple geophones: *Geophysics*, 20, 215-226.
- Lytton, R. L., Moore, W. M., and Mahoney, J. P., 1975, *Pavement evaluation: phase I -- pavement evaluation equipment: FHWA, Rept., FHWA-RD-75-78.*
- Knapp, R. W., 1986, Geophone differencing to attenuate horizontally propagating noise: *Geophysics*, 51, 1743-1759.
- Mari, J. L., 1984, Estimation of static corrections for shear-wave profiling using the dispersion properties of Love waves: *Geophysics*, 49, 1169-1179.

McMechan, G. A., and Yedlin, M. J., 1981, Analysis of dispersive waves by wave field transformation: *Geophysics*, 46, 869-874.

Mokhtar, T. A., Herrmann, R. B., and Russel, D. R., 1988, Seismic velocity and  $Q$  model for the shallow structure of the Arabian shield from short-period Rayleigh waves: *Geophysics*, 53, 1379-1387.

Moore, R. C., 1964, Paleocological aspects of Kansas Pennsylvanian and Permian Cyclothems; *Kansas Geological Bull.*, 169, v. 1, 287-380.

Nazarian, S., Stokoe II, K. H., and Hudson, W. R., 1983, Use of spectral analysis of surface waves method for determination of moduli and thicknesses of pavement systems, *Transportation Research Record No. 930*, 38-45.

Park, C. B., Miller, R. D., and Xia, J., 1996a, Multi-channel analysis of surface waves using Vibroseis, Presented at the 66th Ann. Mtg. of SEG, Denver, Expanded Abstracts, 68-71.

Park, C. B., Xia, J., and Miller, R. D., 1996b, Techniques to calculate phase velocities of surface waves from Vibroseis multi-channel data: Submitted for publication in *Geophysics*.

Park, C. B., Miller, R. D., and Xia, J., 1996c, Multi-channel analysis of surface waves (MASW): Submitted for publication in *Geophysics*.

Park, C. B., Miller, R. D., and Xia, J., 1997a, Multi-channel analysis of surface waves using impulsive source (MASI): in preparation for publication.

Park, C. B., and Miller, R. D., 1997b, Imaging near-surface heterogeneity by surface waves: in preparation for publication.

Park, C. B., Xia, J., and Miller, R. D., 1997c, An approximate inversion method for surface waves: in preparation for publication.

Rix, G. J., and Leipski, E. A., 1991, Accuracy and resolution of surface wave inversion, in *Geotechnical special publication no. 29, Recent advances in instrumentation, data acquisition and testing in soil dynamics*, edited by S. K. Bhatia, S. K. and G. W. Blaney, American Society of Civil Engineers, 17-32.

Sanchez-Salinerio, I., Roesset, J. M., Shao, K. Y., Stokoe II, K. H., and Rix, G. J., 1987, Analytical evaluation of variables affecting surface wave testing of pavements, *Transportation Research Record No. 1136*, 86-95.

Santamarina, J. C., 1994, An introduction to geotomography, in *Geophysical characterization of sites*, ISSMFE Technical Committee #10, edited by R. D. Woods, Oxford Publishers, New Delhi.

Sheu, J. C., Stokoe II, K. H., and Roesset, J. M., 1988, Effect of reflected waves in SASW testing of pavements, Transportation Research Record No. 1196, 51-61.

Stokoe II, K. H., Wright, G. W., James, A. B., and Jose, M. R., 1994, Characterization of geotechnical sites by SASW method, in Geophysical characterization of sites, ISSMFE Technical Committee #10, edited by R. D. Woods, Oxford Publishers, New Delhi.

Yilmaz, O., 1987, Seismic data processing: Doherty, S. M., Ed.: Investigations in Geophysics, no. 2, Soc. of Expl. Geophys.

Xia, J., Miller, R. D., and Park, C. B., 1997, Estimation of near-surface shear-wave velocity by inversion of Rayleigh wave: in preparation for publication.

## FIGURE CAPTIONS

Fig. 1. Basic configurations of (a) Spectral Analysis of Surface Waves (SASW) method and (b) Multi-Channel Analysis of Surface Waves (MASW) method.

Fig. 2. An uncorrelated field record obtained at Kansas Geological Survey (KGS) test site for the purpose of testing multi-channel analysis of surface waves using Vibroseis (MASWV) method.

Fig. 3. (a) Two shear-wave velocity ( $v_s$ ) profiles: one obtained from the inversion of the dispersion curve (shown in Figure 3b) constructed from the field record in Figure 2 by using CCSAS method and another obtained from a down-hole survey. (b) Comparison of the two dispersion curves: one from the field measurement (measured) and another from the inverted  $v_s$  profile (inversion).

Fig. 4. Comparison of dispersion curves obtained by using two different data processing techniques used in MASWV and MASWI methods, respectively.

Fig. 5. (a) Velocity models used for test of the imaging method by surface waves and (b) corresponding dispersion curves.

Fig. 6. An uncorrelated field record modeled for test of the imaging method showing the signature of abnormal zone before and after linear moveout (LMO) correction.

Fig. 7. Common-receiver gathers for two receiver locations: one located above a normal zone and another located above an anomaly zone.

Fig. 8. Stacked section of the common-receiver gathers showing the presence of the anomaly as a "white" spot.

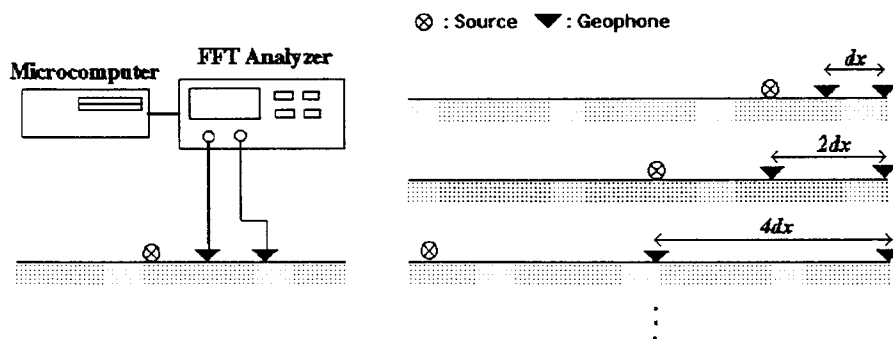
Fig. 9. Real data example of the stacked section obtained by the imaging method.

Fig. 10. A schematic illustration of the case in which MASW method uses a receiver platform. The platform consists of multiple number of receivers mounted on a fairly heavy and homogeneous frame that can be pulled by men or a vehicle.

Fig. 11. A schematic illustration to show feasibility of tomographic imaging by surface waves. Assuming an isotropic elastic property of earth, different depths of near-surface can be oversampled by surface wave of a certain wavelength propagating in different directions through the same part of the medium. Therefore, one can have an overdetermined matrix equation to be solved for either dispersion data or shear-wave velocity with much a higher accuracy than would be achieved by any other method.

(a)

## Spectral-Analysis-of-Surface-Waves (SASW)



(b)

## Multi-Channel Analysis of Surface Waves (MASW)

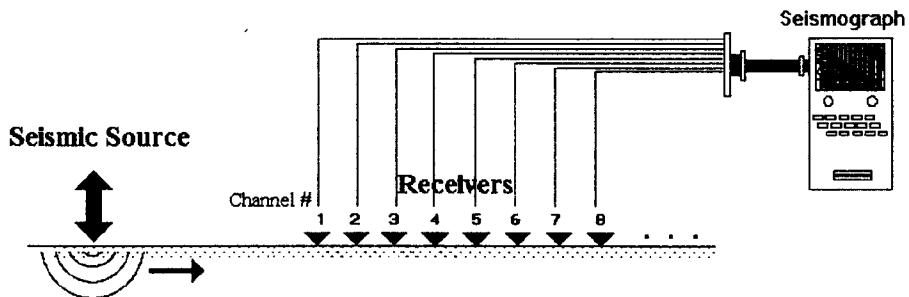


Fig. 1.

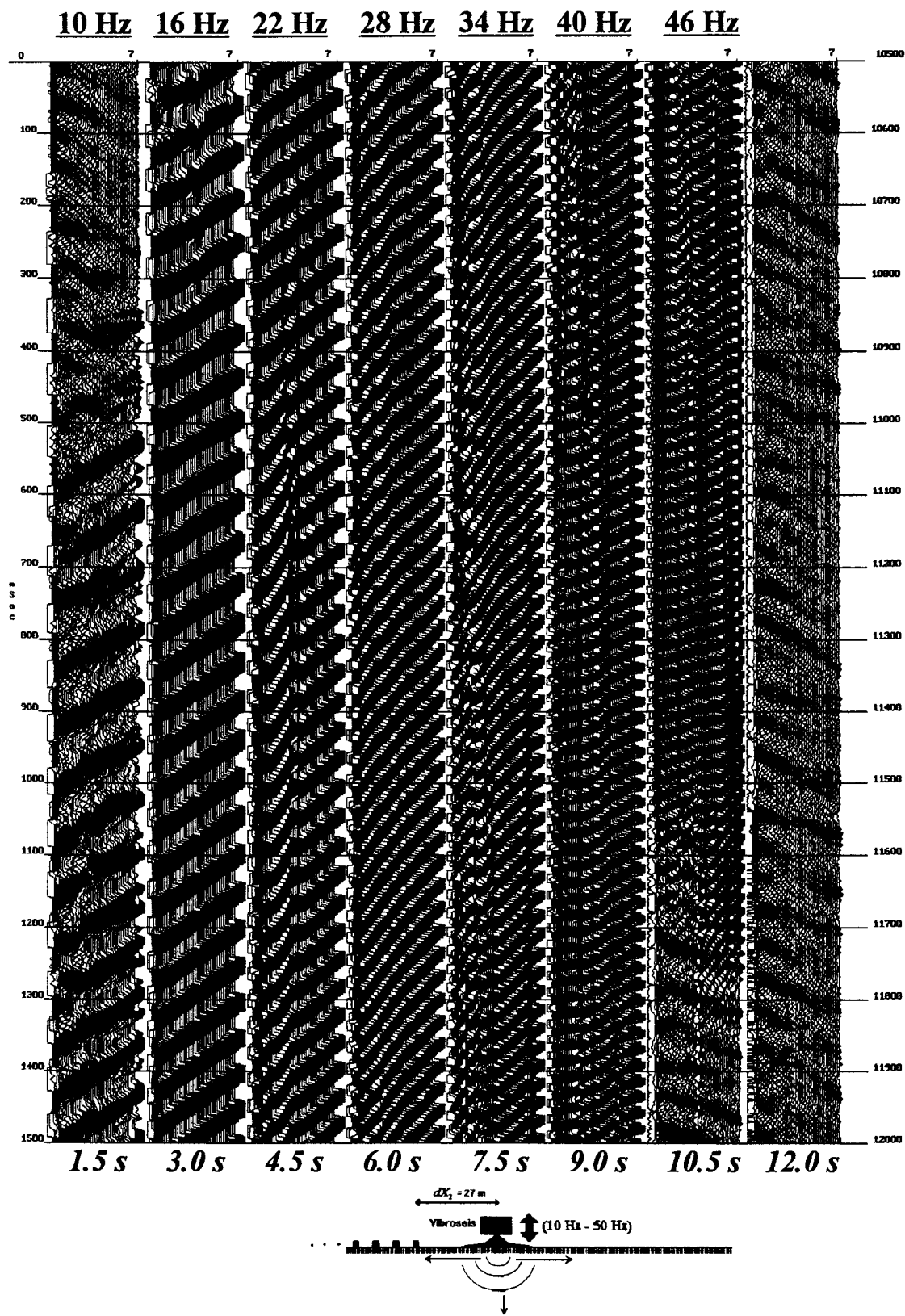
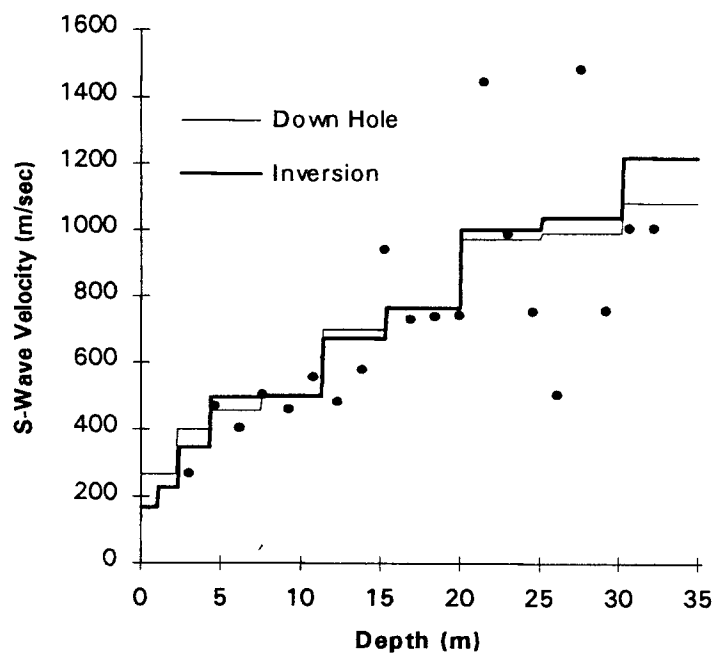


Fig. 2.

(a)



(b)

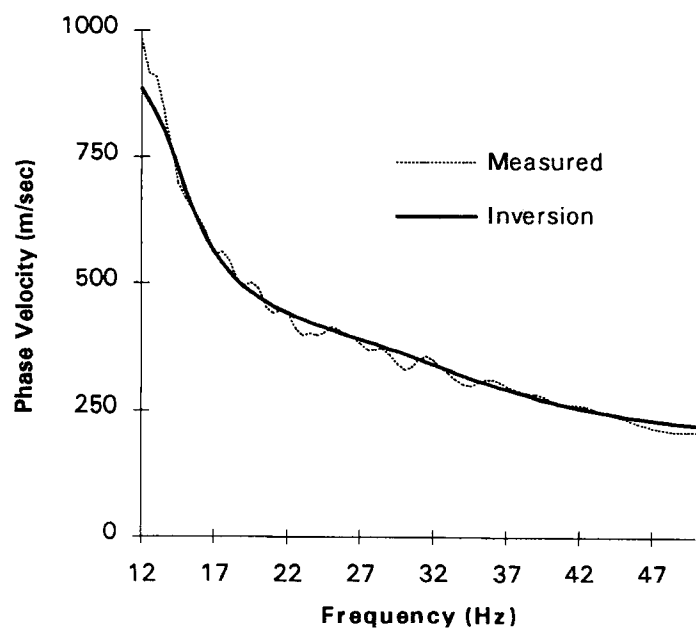


Fig. 3.

## Comparison of *MSAWV* and *MASWI* with Vibroseis Data

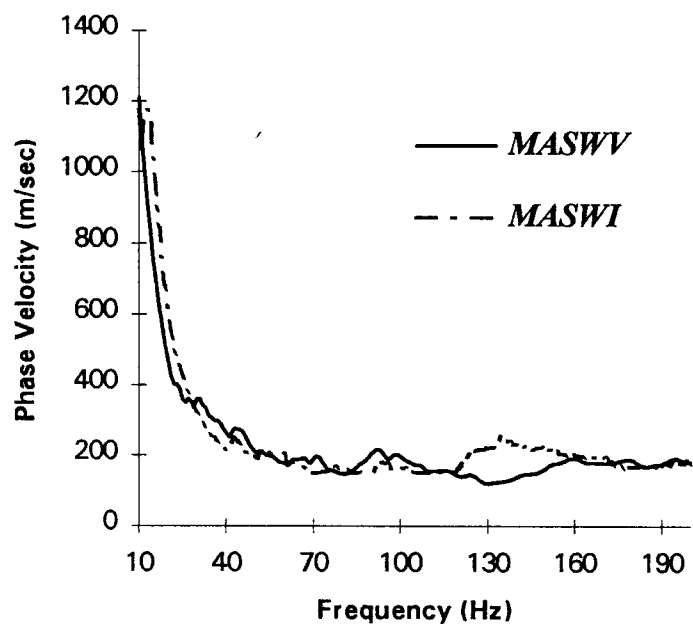
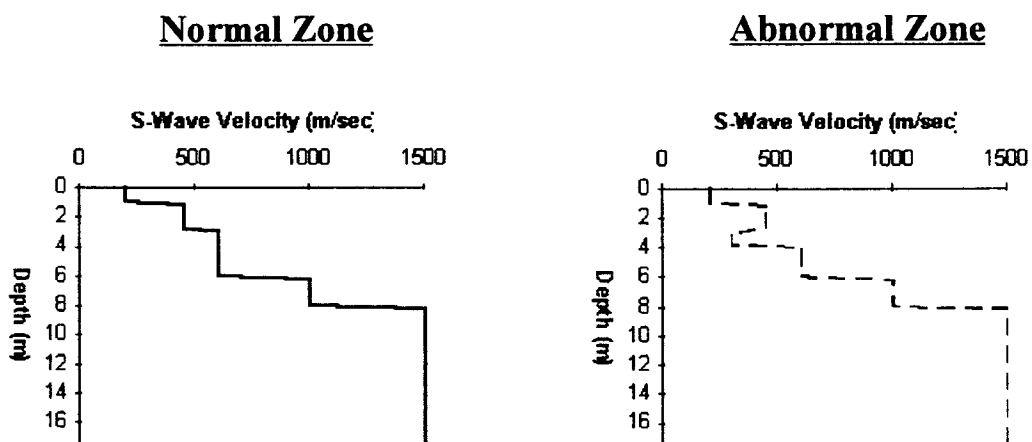


Fig. 4.

(a)



(b)

### Dispersion Curves

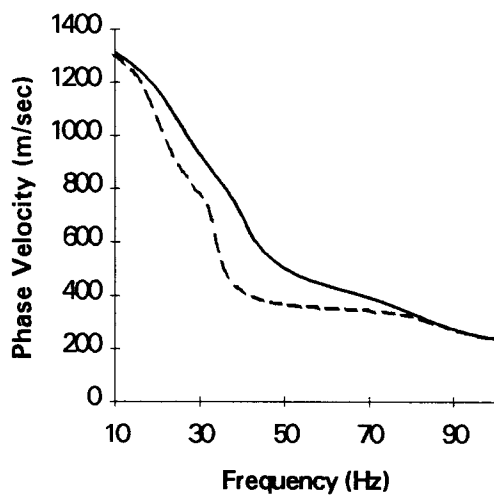
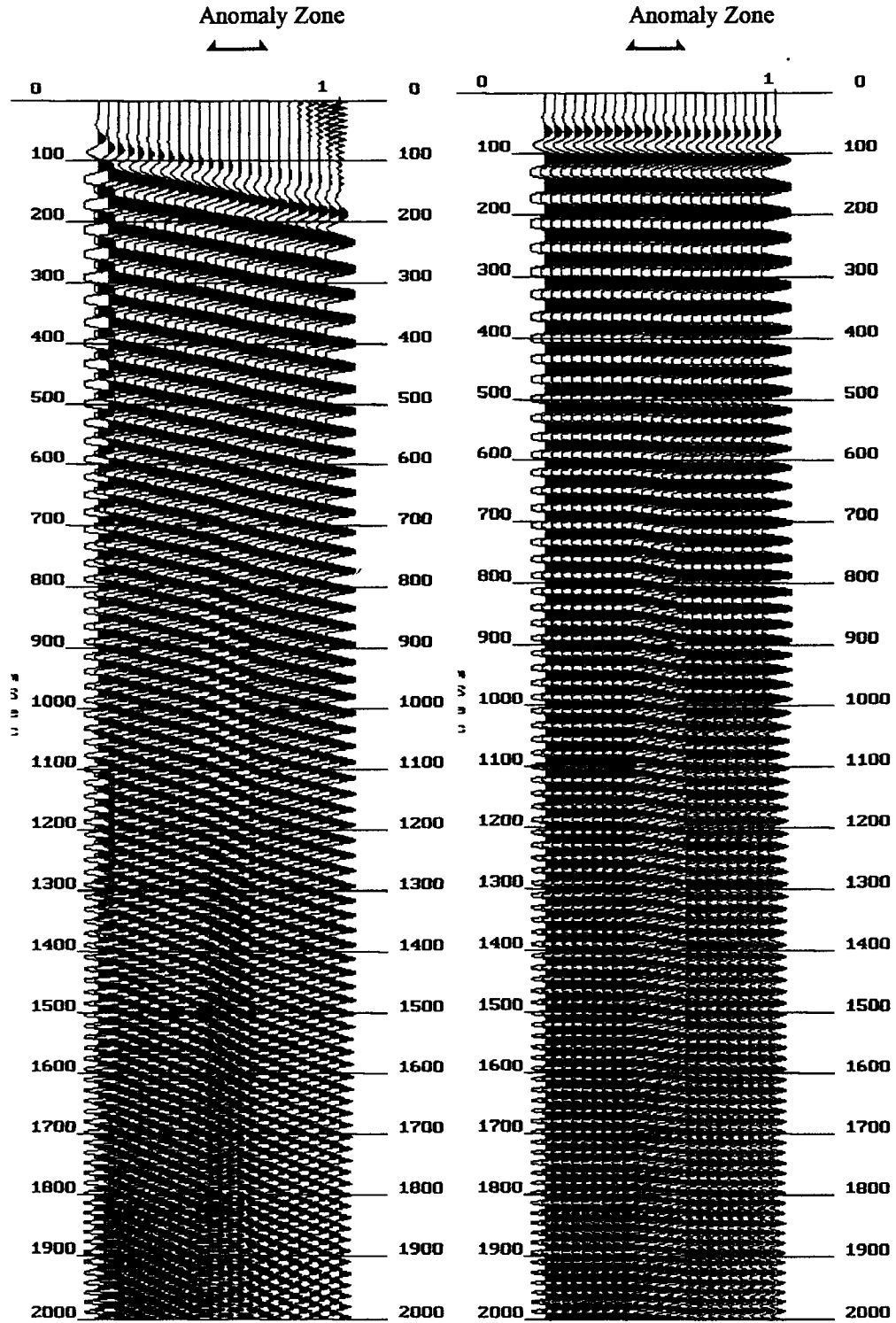


Fig. 5.

**Before LMO Correction**

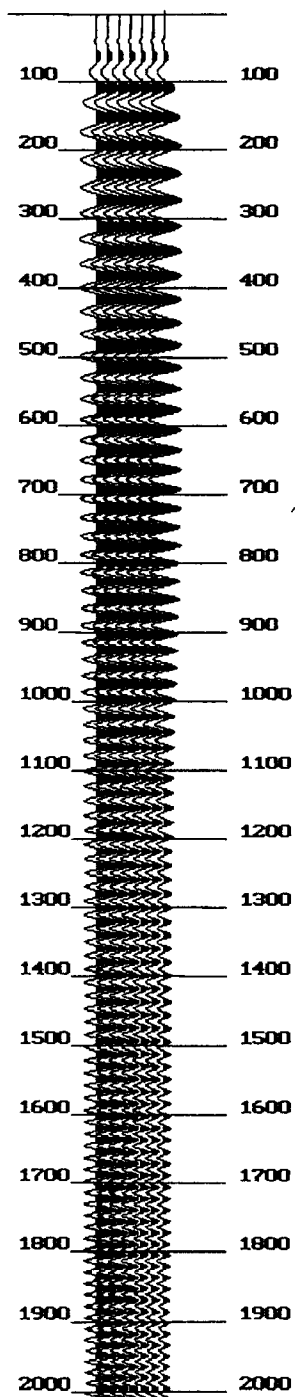
**After LMO Correction**



**Fig. 6.**

## Common-Receiver Gathers

### Above Normal Zone



### Above Abnormal Zone

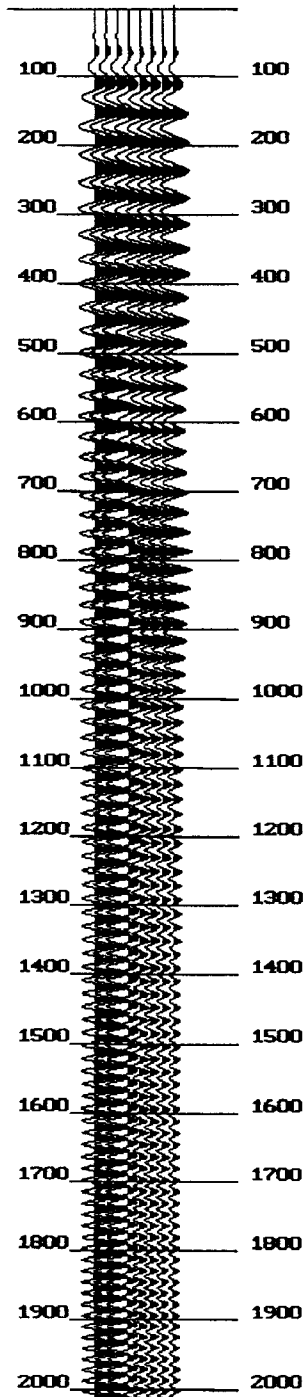


Fig. 7.

## Stacked Section (Modeling Result)

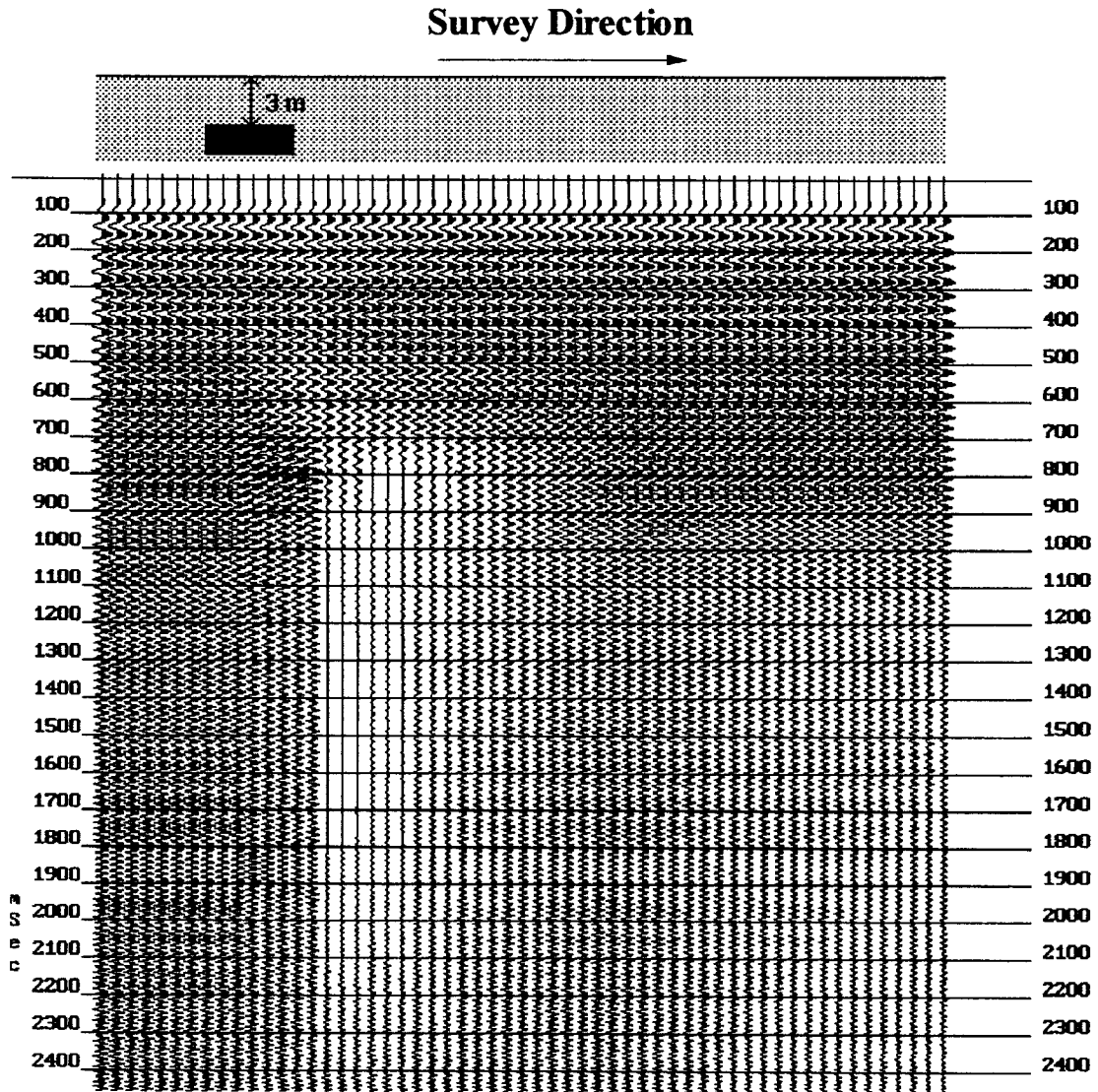
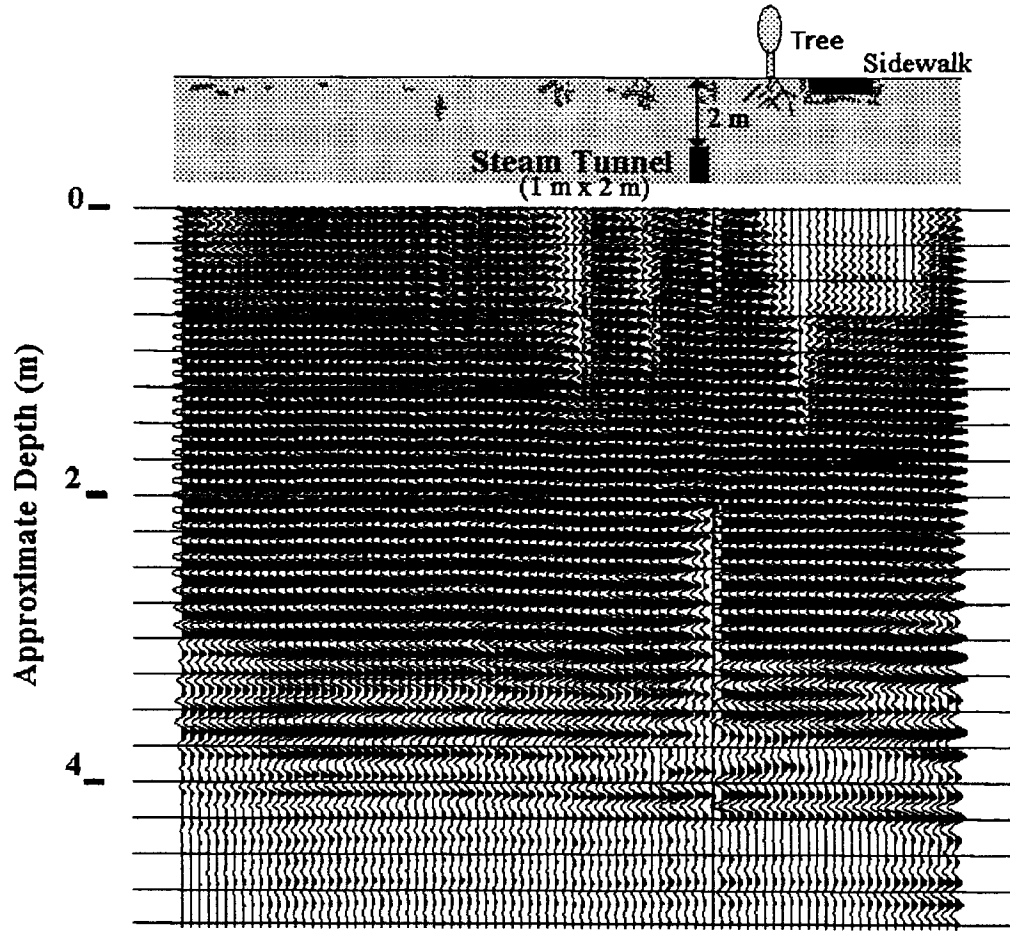


Fig. 8.

# Stacked Section (Field Result)



**Fig. 9.**

## **MASW IN RECEIVER PLATFORM**

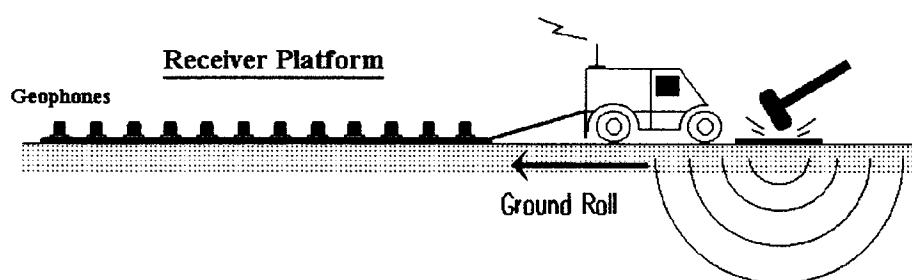


**Fig. 10.**

## FEASIBILITY OF TOMOGRAPHIC IMAGING BY *MASW*

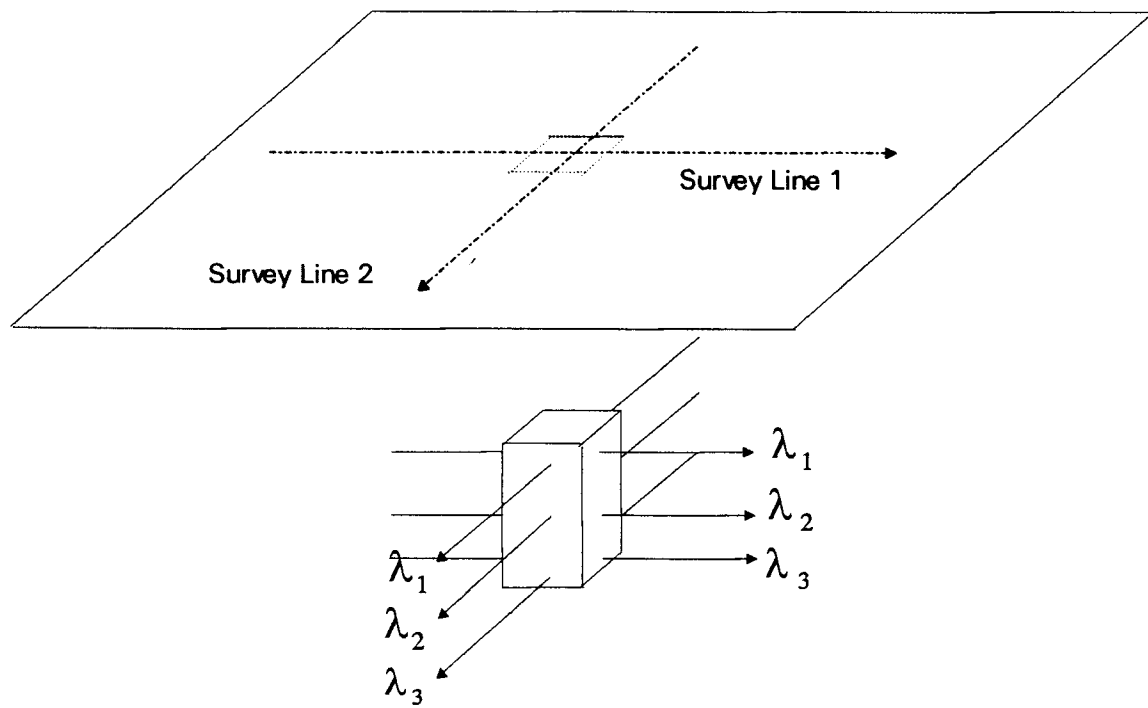


Fig. 11.